

Article

High-Resolution Millimeter-Wave Radar for Real-Time Detection and Characterization of High-Speed Objects with Rapid Acceleration Capabilities

Yair Richter and Nezah Balal * 

Department of Electrical and Electronic Engineering, Faculty of Engineering, Ariel University, Ariel 40700, Israel
* Correspondence: nezahb@ariel.ac.il

Abstract: In this study, we present a novel approach for the real-time detection of high-speed moving objects with rapidly changing velocities using a high-resolution millimeter-wave (MMW) radar operating at 94 GHz in the W-band. Our detection methodology leverages continuous wave transmission and heterodyning of the reflected signal from the moving target, enabling the extraction of motion-related attributes such as velocity, position, and physical characteristics of the object. The use of a 94 GHz carrier frequency allows for high-resolution velocity detection with a velocity resolution of 6.38 m/s, achieved using a short integration time of 0.25 ms. This high-frequency operation also results in minimal atmospheric absorption, further enhancing the efficiency and effectiveness of the detection process. The proposed system utilizes cost-effective and less complex equipment, including compact antennas, made possible by the low sampling rate required for processing the intermediate frequency signal. The experimental results demonstrate the successful detection and characterization of high-speed moving objects with high acceleration rates, highlighting the potential of this approach for various scientific, industrial, and safety applications, particularly those involving targets with rapidly changing velocities. The detailed analysis of the micro-Doppler signatures associated with these objects provides valuable insights into their unique motion dynamics, paving the way for improved tracking and classification algorithms in fields such as aerospace research, meteorology, and collision avoidance systems.

Keywords: Doppler radar; millimeter wave radar; real-time detection; low sampling rate; high-resolution velocity detection; civilian applications; aerospace research; meteorology; collision avoidance systems



Citation: Richter, Y.; Balal, N. High-Resolution Millimeter-Wave Radar for Real-Time Detection and Characterization of High-Speed Objects with Rapid Acceleration Capabilities. *Electronics* **2024**, *13*, 1961. <https://doi.org/10.3390/electronics13101961>

Academic Editor: Flavio Canavero

Received: 3 March 2024

Revised: 9 May 2024

Accepted: 13 May 2024

Published: 16 May 2024



Copyright: © 2024 by the authors. Licensee MDPI, Basel, Switzerland. This article is an open access article distributed under the terms and conditions of the Creative Commons Attribution (CC BY) license (<https://creativecommons.org/licenses/by/4.0/>).

1. Introduction

Conventional microwave radar systems face significant challenges in accurately detecting and tracking high-speed moving objects, particularly those with rapidly changing velocities [1–3]. The primary difficulty lies in resolving the substantial Doppler shifts caused by the rapid motion of these objects, leading to inaccuracies in both detection and tracking. Traditional radar systems, which are typically ground-based and stationary, struggle to effectively capture the complex dynamics of fast-moving targets due to their limited frequency resolution and inability to account for the unique micro-Doppler signatures associated with these objects [4–7].

Recent studies have explored various aspects of detecting and characterizing high-speed, low-RCS targets using radar systems, with a focus on civilian applications such as space exploration, meteorology, and safety systems. For example, Chen et al. [8] investigated the micro-Doppler effect in radar and its potential for target classification, while Ren et al. [9] proposed a deep learning approach for micro-Doppler signature analysis. Additionally, Wang et al. [10] examined the use of millimeter-wave radar for the detection and tracking of small UAVs, highlighting the challenges associated with low-RCS targets. These studies underscore the growing interest in developing advanced radar systems

capable of detecting and characterizing high-speed, low-RCS targets for a wide range of non-military applications.

This study presents an innovative solution utilizing high-resolution millimeter-wave (MMW) radar systems operating in the W-band at 94 GHz. While conventional radar systems often operate in the ultra-high frequency (UHF) band, typically defined as 300 MHz to 3 GHz, the W-band offers significantly higher frequency resolution, enabling more accurate detection and characterization of high-speed targets, especially those exhibiting rapid velocity changes. MMW radars demonstrate superior capabilities in detecting the complex motion of aerial targets, including the rotating and vibrating components characteristic of advanced propulsion systems [11,12]. These motion-induced micro-Doppler effects, often indistinguishable at lower frequencies, are critical for enhancing the detection and characterization of such targets, thereby significantly improving radar performance in civilian applications involving objects with high acceleration rates [13,14].

This research examines the unique challenge posed by high-speed moving objects with rapidly changing velocities and proposes an advanced radar detection system designed for high-resolution velocity measurements and improved resilience to atmospheric interference. The proposed system addresses a longstanding issue in radar detection for scientific and industrial purposes, particularly in applications where the targets exhibit significant and rapid velocity variations [15,16].

Building upon the foundational work of previous studies [13,14,17], our methodology harnesses continuous wave (CW) transmission combined with sophisticated signal processing techniques. This approach enables accurate capture of the motion characteristics of high-speed targets. We validate the efficacy of our technique through systematic experiments and simulations, providing a comprehensive analysis of the radar system's capabilities in detecting and tracking objects with high acceleration rates. The choice of appropriate sampling windows and spectrogram analysis is crucial for effectively tracking the velocity variations of the object over time, aligning with the principles of micro-Doppler analysis [18]. By applying these techniques to the high-resolution data obtained from the MMW radar, we can extract detailed micro-Doppler signatures that provide valuable insights into the unique dynamics of high-speed moving objects.

Our research significantly contributes to the field by enhancing the efficiency and reliability of radar systems for critical civilian applications [19–22]. This study addresses a vital gap in current radar technology and paves the way for future advancements in detecting and characterizing high-speed moving objects using advanced MMW radar techniques [23]. By providing a more comprehensive understanding of the micro-Doppler signatures associated with these objects, our work enables the development of more effective detection and tracking algorithms, ultimately improving the performance and capabilities of radar systems in a wide range of applications.

2. Continuous Wave Micro-Doppler Radar

The continuous wave (CW) micro-Doppler radar system depicted in Figure 1 operates by transmitting a millimeter-wave signal at a fixed carrier frequency f_0 . The signal, represented by (1), is a sine wave modulated by the following carrier frequency:

$$E_t(t) = \text{Re}\left\{A_t e^{j2\pi f_0 t}\right\} \quad (1)$$

Once reflected off a moving target, this signal is received as a signal whose frequency has been shifted due to the Doppler effect. The received signal, shown in (2), incorporates the effects of target movement:

$$E_r(t) = \text{Re}\left\{A_r e^{-j(2kR(t)+\theta)} e^{j2\pi f_0 t}\right\} \quad (2)$$

In these expressions, A_t and A_r are the amplitudes of the transmitted and received signals, respectively. The wavenumber k is defined as $2\pi f_0 / c$, where c is the speed of light.

The variable $R(t)$ denotes the distance to the moving target, and θ represents the phase shift induced by the reflection process.

The detection mechanism of the radar involves heterodyning, which is the process of mixing the transmitted signal with the received signal. This yields a product, as shown in (3), which isolates the change in phase due to the target’s motion:

$$\tilde{Z}(t) = A_t A_r e^{j(2kR(t) - \theta)} \tag{3}$$

The phase $\varphi(t)$ of this signal varies with time, as represented by (4):

$$\varphi(t) = 2kR(t) - \theta \tag{4}$$

The phase of this signal varies over time due to the movement of the target.

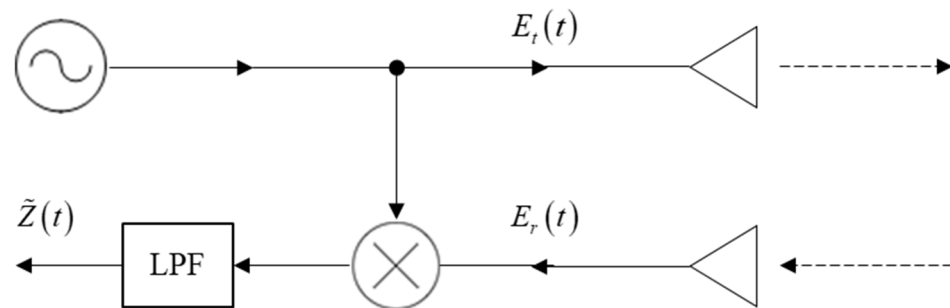


Figure 1. CW micro-Doppler radar.

3. The Influence of Carrier Frequency on Speed Detection

In radar systems, the intricacies of detecting rapid changes in target speed hinge on the physical relationship between the carrier frequency, the Doppler frequency, and the integration time. This relationship plays a pivotal role in the system’s velocity resolution—the ability to discern minute differences in target speed. The carrier frequency, especially when low, can hamper the radar’s sensitivity to speed changes, as the Doppler frequency shift is proportionally related to it. By differentiating the phase, $\varphi(t)$, in (4) with respect to time, we obtain the Doppler frequency shift, as indicated in (5). This frequency shift is a measure of the target’s velocity relative to the radar:

$$f_d(t) = \frac{1}{2\pi} \frac{\partial \varphi(t)}{\partial t} = \frac{1}{2\pi} 2k \cdot \dot{R}(t) = \frac{2f_0}{c} \cdot v_R(t) \tag{5}$$

The Doppler frequency, $f_d(t)$, is crucial for determining the target’s speed. The radar’s ability to resolve different speeds, known as the velocity resolution, depends on the integration time, Δt_I , which is defined by the uncertainty principle in (6):

$$\Delta f_d = \frac{1}{\Delta t_I} \tag{6}$$

The integration time is the time during which the radar signal is processed to detect motion. From (5), we see that the minimum integration time necessary for detecting velocity changes is inversely proportional to the carrier frequency:

$$\frac{1}{\Delta t_I} = \frac{2f_0}{c} \cdot \Delta v_r \tag{7}$$

This implies that higher carrier frequencies allow for a more compact integration time window, which is advantageous for detecting high-speed objects. The higher the frequency, the greater the sensitivity of the radar to changes in the target’s velocity, enabling the radar to track and measure the speed of fast-moving targets quickly and accurately. Conse-

quently, a radar system with a higher carrier frequency in the MMW band can achieve a finer velocity resolution within a shorter integration time, facilitating the detection of rapid speed changes. Conversely, a lower carrier frequency necessitates a longer integration time to achieve the same velocity resolution, which may not be practical for fast-moving targets. Selecting a suitable carrier frequency is crucial when designing radar systems for applications requiring high-velocity resolution, such as tracking objects with rapid acceleration capabilities. Employing MMW frequencies enables the radar to capture complete Doppler cycles within a constrained integration time, making it a superior choice for accurately monitoring high-speed objects. The physical interplay between integration time, velocity resolution, and carrier frequency emphasizes the necessity of MMW radar systems for effective detection and tracking of targets exhibiting high-speed variations and rapid acceleration.

The 3D visualization in Figure 2 depicts the relationship between carrier frequency, velocity resolution, and integration time for a radar system. The horizontal plane combines carrier frequency, ranging from 10 to 100 GHz, with velocity resolution spanning from 0.1 to 1 m/s. The rise from this plane is the integration time, measured in milliseconds. The surface shape and color gradients illustrate that higher carrier frequencies allow shorter integration times to achieve a given velocity resolution. This is a fundamental characteristic of radar systems, where higher frequencies enable more precise and quicker detection capabilities. The contour lines overlaid on the surface further emphasize this relationship, clearly delineating regions of constant integration time and making the trend visually explicit: as we move towards higher frequencies, the required integration time to maintain the same velocity resolution decreases. This graph effectively conveys the advantage of operating at higher frequencies for efficient radar tracking and detecting high-speed targets with rapid acceleration capabilities.

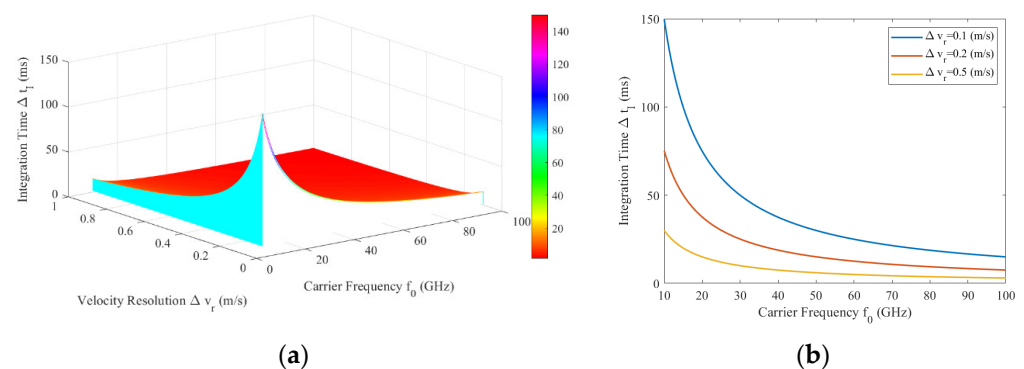


Figure 2. (a) 3D surface plot illustrating the relationship between carrier frequency, velocity resolution, and integration time of the radar system. The graph demonstrates how higher carrier frequencies enable shorter integration times to maintain precise velocity resolution. (b) 2D graph depicting the inverse relationship between carrier frequency and required integration time for a fixed velocity resolution of 0.1, 0.2, and 0.5 (m/s). As the carrier frequency increases, the required integration time decreases, highlighting the advantage of higher frequencies in detecting high-speed targets.

To emphasize the advantage of higher carrier frequencies in detecting high-speed targets, Figure 2b presents a 2D graph illustrating the relationship between the carrier frequency and the required integration time for a given velocity resolution. As the carrier frequency increases, the required integration time decreases, following an inverse relationship. This trend highlights the crucial role of higher frequencies in enabling shorter integration times, which are essential for accurately tracking rapid changes in target velocity. By operating at higher carrier frequencies, such as those in the millimeter-wave range, radar systems can achieve the necessary velocity resolution while maintaining short integration times, making them well suited for detecting and tracking high-speed targets.

Selecting an appropriate STFT window length is crucial for effectively capturing the micro-Doppler signatures associated with rapid velocity changes in high-speed objects with

rapid acceleration capabilities. By carefully choosing the window length, it is possible to balance frequency and temporal resolution. Using a high-frequency millimeter-wave radar operating at 94 GHz in this study enables the detection of subtle velocity variations over extremely short time intervals. This is due to the direct relationship between the carrier frequency and the Doppler frequency shift, as described by Equation (5). Consequently, high-frequency radar allows for shorter STFT windows while maintaining sufficient frequency resolution to resolve micro-Doppler signatures. This combination of high carrier frequency and an optimized STFT window enables the system to capture and distinguish the unique micro-Doppler signatures associated with the rapid acceleration and deceleration of high-speed objects, even when these velocity changes occur over brief periods. The ability to detect these subtle variations in velocity is essential for accurate characterization of the motion of a target and highlights the advantages of employing a high-resolution MMW radar system for this purpose. Similar principles have been successfully applied in other domains, such as fall detection using micro-Doppler millimeter-wave radar [24], demonstrating the versatility and potential of this approach for civilian applications.

4. High-Speed Object Trajectories and Experimental Setup

Objects propelled by high-acceleration propulsion systems are known for their high speed and unique flight characteristics, particularly their ability to achieve rapid velocity changes. Understanding and detecting these objects is crucial for various civilian applications, including aerospace research, space exploration, and safety systems. The object's motion can be described in two stages (Figure 3). Initially, a propulsive force accelerates the object, achieving an initial speed of approximately 100 m/s. In the second stage, the object further accelerates to 250 m/s at a distance of 20 m from the launch point, demonstrating its capability for swift velocity changes. The propulsion system operates up to approximately 100 m before disengaging, after which the speed gradually decreases until the object either reaches its intended destination or comes to rest.

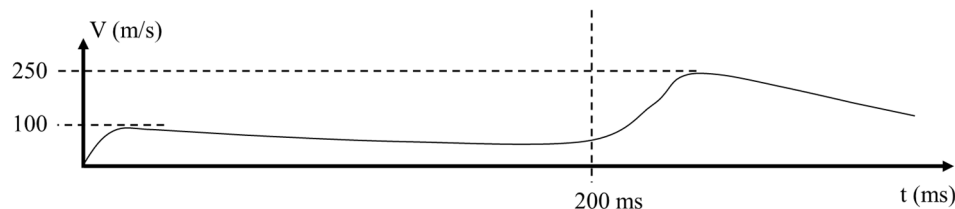


Figure 3. Diagram illustrating the operational stages of a high-acceleration propulsion system and the corresponding speed of the object as a function of time. The graph demonstrates the object's ability to achieve rapid velocity changes during its flight.

Understanding the unique flight characteristics of high-speed objects with rapid acceleration capabilities is crucial for various applications, including aerospace research, space exploration, safety systems, and air traffic management. These objects exhibit distinct velocity profiles and acceleration patterns that impact their detection, tracking, and prediction. Accurate knowledge of their flight dynamics, particularly their ability to undergo sudden velocity changes, is essential for designing propulsion systems, developing trajectory models, establishing safety protocols, and ensuring the safe operation of civilian aircraft and spacecraft. By providing insights into the flight characteristics of high-speed objects with rapid acceleration, this research contributes to advancing knowledge in these fields and enables the development of more sophisticated systems for detecting, tracking, and managing these objects in civilian contexts. Accurate detection and tracking of high-speed objects using radar technology have various applications, such as in aerospace research, space exploration, and safety systems. However, detecting these objects poses challenges due to their time-varying speed and short detection time, given the high velocities involved.

Prior to the radar measurements, a single launch experiment was conducted to validate the radar's velocity detection capabilities. High-speed cameras were positioned along the object's trajectory to capture its motion during the launch. The recorded video footage was

analyzed to extract the object's position as a function of time. These position measurements were then numerically differentiated to obtain the velocity profile of the object. The resulting velocity data served as a reference for comparison against the radar-based measurements.

The radar output is analog, necessitating the selection of an appropriate sampling frequency. This frequency was determined based on the Doppler radar Equation (5). The maximum anticipated detection speed of 250 m/s corresponds to a radar output frequency of 160 kHz. In adherence to the Nyquist criterion, a sampling frequency of 2 MHz, which is more than ten times the expected frequency, was chosen.

To prevent damage, the radar was positioned adjacent to the expected object path rather than facing the launch line. A slight deviation in the radar's placement along the object's trajectory increased its range. The radar system records data in response to a trigger, which is subsequently analyzed on a computer after the launch event (Figure 4).

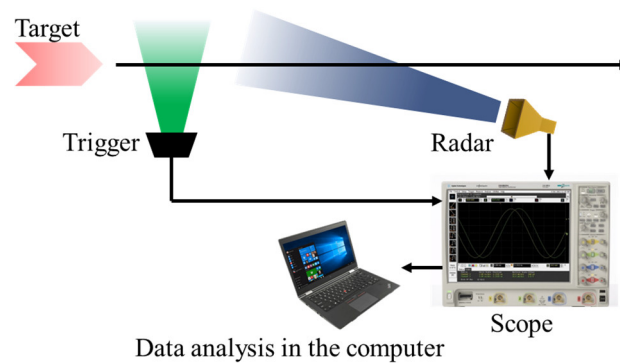


Figure 4. Schematic of the experimental system showing the radar placement adjacent to the expected object path, with a slight deviation to increase range and prevent damage.

Understanding the influence of antenna characteristics on radar detection capabilities is crucial for interpreting the experimental results. The antenna's gain, G , is closely related to its effective aperture area, A_e , which depends on both the physical size and the efficiency of the antenna, as given by the following:

$$G = \frac{4\pi A_e}{\lambda^2} \quad (8)$$

where λ represents the wavelength of the radar's operational frequency. The effective aperture, A_e , is derived from the antenna's physical area, A , and its efficiency, η , as follows:

$$A_e = \eta A \quad (9)$$

The beamwidth, Θ , which indicates the antenna's angular coverage, is inversely proportional to the square root of the antenna's gain. For a parabolic antenna with a circular aperture, D , the beamwidth is approximated by the following:

$$\Theta \approx \frac{70\lambda}{D} \quad (10)$$

Similarly, for rectangular horn antennas, the beamwidth is determined by the aperture dimensions in the E-plane and H-plane.

For rectangular horn antennas (Figure 5), the beamwidth calculations are based on the dimensions of the aperture in both the E-plane and the H-plane:

$$\Theta_E \approx \frac{\lambda}{l_E} \text{ and } \Theta_H \approx \frac{\lambda}{l_H} \quad (11)$$

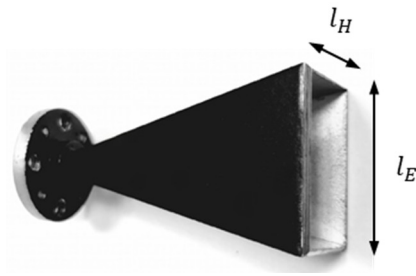


Figure 5. Horn antenna schematic for system dimension stabilization and main lobe radiation angle calculation. This diagram depicts a horn antenna used to determine the system’s dimensions and to calculate the radiation angle within the main lobe, which is critical for accurate beam alignment and signal detection.

These relationships highlight the trade-offs between antenna gain, aperture size, and beamwidth. A higher gain antenna will have a narrower beamwidth, concentrating the radar energy over a smaller angular region, which can enhance detection of targets within that region but may limit the overall coverage area. Conversely, a lower gain antenna will have a wider beamwidth, providing broader angular coverage at the expense of reduced sensitivity in any specific direction.

Our experimental methodology was designed to investigate these trade-offs and their impact on the detection of high-acceleration objects using antennas with different characteristics.

5. Radar Detection and Analysis of High-Speed Object Trajectories and Measurement Results

In this section, we present the results of our experimental study on detecting and tracking high-speed objects with rapid acceleration capabilities using a high-resolution millimeter-wave radar system. The results are organized into subsections, each focusing on a specific aspect of the radar’s performance and the object’s motion characteristics. We provide detailed explanations of our data processing techniques and analysis methods to ensure their clarity and reproducibility. Additionally, we have included visual aids, such as graphs and diagrams, to support the textual descriptions and facilitate a better understanding of the key findings. The radar system was placed 84 m from the launch point and tasked with detecting the launch of the objects. To capture the full breadth of the radar’s response, the scope’s buffer was configured to record data spanning from 100 milliseconds before to 900 milliseconds after an optical system triggered, corresponding to each launch event, providing a comprehensive one-second data window for each measurement.

The radar system used operates at 94 GHz with a transmit power of 10 dBm and a noise figure of 5 dB. Three different antennas were utilized in the experiments. Table 1 summarizes the experimental setup details for each radar measurement, including antenna type, dimensions, beamwidth, and gain.

Table 1. Details of the experimental setup for the radar measurements, including antenna type, beamwidth, and gain.

Antenna Type	Antenna Beamwidth (Degrees)	Antenna Gain (dBi)	Measurement Number (#)
parabolic	3×3	30	#1
rectangular horn	8×8	18	#2–#5
rectangular horn	30×30	15	#6

Six object launch measurements were conducted with the radar. A sample spectrogram of measurement #2 evidencing these capabilities is depicted in Figure 6. Measurements #2–#5 utilizing the medium-gain antenna enabled detailed detection and velocity profile analysis of

the object over time (Figure 7). The medium-gain antenna provided a suitable combination of beamwidth and gain to achieve an adequate signal-to-noise ratio (SNR) for detecting the object. The linear velocity profile observed in Figure 7b corresponds to the second stage of the object’s trajectory, where it experiences nearly constant acceleration. This stage is of particular interest to our research, as the high acceleration and rapid change in velocity pose significant challenges for radar detection and tracking systems. Accurately capturing and analyzing the velocity profile during this critical phase is essential for developing effective tracking algorithms and improving the overall performance of radar systems in detecting and tracking high-speed objects with rapid acceleration. Subsequent employment of the high-gain antenna in meas. #1, with its narrow 3×3 degree beamwidth, increased the maximum detection range, as indicated in Figure 6, as a result of the shorter detection time. This extended range likely stems from the higher antenna gain concentrating more energy on the target, improving the SNR. Although theory constrains the angular coverage of such a narrow beamwidth, the precise orientation aligns the antenna pattern with the object’s trajectory in this case. Measurement #6, which leverages the low-gain antenna, failed to detect the object. The substantial 30×30 degree beamwidth spreads radar energy over a wider area, drastically lowering the SNR. This highlighted the severe sensitivity loss when power is dispersed across an amplified angular sector. In summary, the empirical results validate the conceptual model and accentuate the delicate tradeoff necessitated between an antenna’s gain, beamwidth, orientation, and SNR when designing optimal radar systems for detecting and tracking high-speed objects with rapid acceleration capabilities.

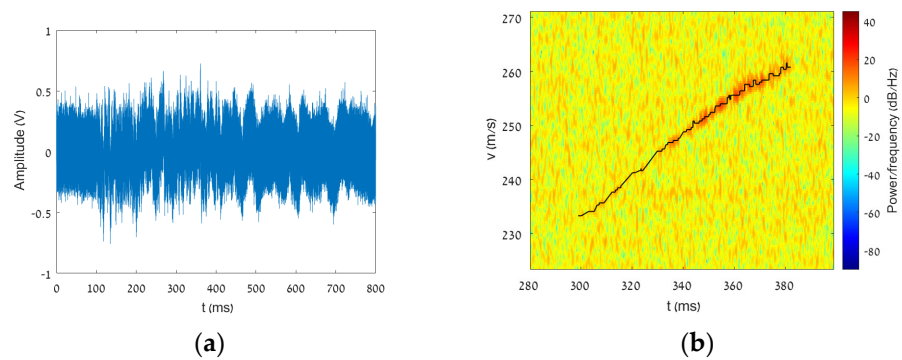


Figure 6. Integrated Radar Analysis Workflow (a) IF Signal Acquisition: This segment captures the radar’s detection phase, where the intermediate frequency (IF) signal is measured directly after being reflected from the object. (b) Threshold Application: Depiction of the threshold level is applied to the spectrogram data to discern between signal and noise, highlighting the significant spectral events indicative of the object’s movement.

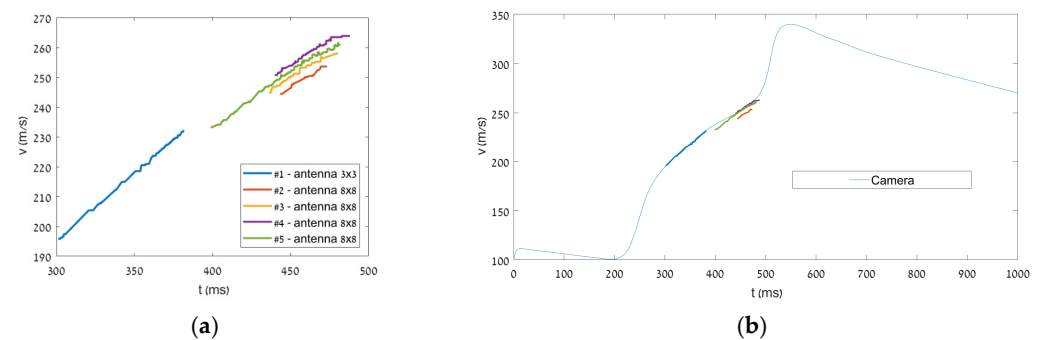


Figure 7. (a) Concentrated results of radar measurements after applying a threshold filter, emphasizing critical spectral data corresponding to the detected motion of the object as a function of time. (b) Velocity profile of the object as a function of position obtained from the high-speed camera and the radar system. The camera-based velocity profile serves as the ground truth for validating the radar measurements, which are derived by integrating the velocity data as a function of time.

6. Streamlined RCS Measurement Method Using a Radar System

Accurate measurement of the Radar Cross Section (RCS) is crucial for characterizing the reflectivity and detectability of objects in radar systems. Estimating the RCS size is essential for ensuring an adequate channel balance and determining the amount of returned power, which helps to adjust system parameters such as transmit power and antenna sizes. Traditional RCS measurement methods often require specialized facilities and expensive setups, limiting their accessibility and practicality. In this section, we propose a streamlined RCS measurement technique using a spectrum analyzer and a continuous wave (CW) source, employing the same radar system used for detecting and tracking high-speed objects. This approach simplifies the RCS measurement process, reduces costs, and ensures high compatibility between the measured RCS values and the actual detection capabilities of the radar system. By providing a cost-effective and efficient method for RCS measurement, this section contributes to the overall understanding and characterization of the objects being detected and tracked by the proposed radar system, ultimately aiding in the optimization of the radar system's performance.

The RCS is crucial in radar technology because it represents the target's effective area that reflects radar signals back towards the source. Expressed in square meters (m^2) or decibels relative to a square meter (dBsm), the RCS characterizes a target's radar visibility. Typically, an RCS is displayed using 2D or 3D graphs across various planes, including azimuth and elevation, or in Cartesian coordinates.

The RCS directly influences the power received by the radar, as detailed in the radar equation:

$$P_r = \frac{P_t G_t G_r}{(4\pi)^3 R^4} \sigma \quad (12)$$

Here, P_r is the received power, P_t is the transmitted power, G_t and G_r are the transmit and receive antenna gains, R is the target distance, and σ is the RCS.

In static scenarios where neither the radar nor the target moves, this equation simplifies to the following:

$$P_r = K\sigma \quad (13)$$

where K is a constant incorporating all other fixed parameters. Understanding a target's RCS is vital for enhancing radar-based detection, identification, and tracking. This approach is also key in designing objects such as stealth aircrafts, which aim to minimize radar visibility. Traditional RCS measurements require specialized antenna ranges and an expensive setup involving large rooms with specially coated walls to minimize extraneous signals. Our study introduces a cost-effective RCS measurement technique using the radar system itself. By calibrating a constant K from (13), we eliminate the need for elaborate setups and coatings.

Calibration begins with a metal sphere of known radius A , providing a calculable RCS:

$$\sigma_{\text{sphere}} = \pi A^2 \quad (14)$$

By measuring the radar's received power from this sphere at a known distance R , we determine K :

$$K = \frac{P_r(\text{sphere})}{\sigma_{\text{sphere}}} \quad (15)$$

By replacing the sphere with the target object, we can then measure the target's RCS directly using the calibrated system. To account for environmental factors, we subtract the power received in free space (FS) from that received with the target:

$$\sigma = \frac{P_r - P_r(\text{FS})}{K} \quad (16)$$

In Equation (16), P_r represents the total power received by the radar when the target is present, which includes both the power reflected by the target and any background noise

or interference. $P_r(\text{FS})$ represents the power received in free space, which is measured without any target or calibration object present. This “free space” measurement accounts for the background noise and interference in the environment.

By subtracting $P_r(\text{FS})$ from P_r , we effectively isolate the power specifically reflected by the target, removing any contributions from background noise or interference. This subtraction ensures that the RCS measurement, σ , accurately represents the target’s reflectivity, independent of environmental factors.

This approach ensures high compatibility between RCS measurements and actual target detection, as the same radar system is used for both. This approach simplifies the RCS measurement process, making it accessible with existing radar systems without the need for specialized facilities.

The proposed method was assessed with a system consisting of a transmitter with a transmission frequency of 94 GHz and a spectrum device that measures the returned power from the target, as presented in Figure 8.

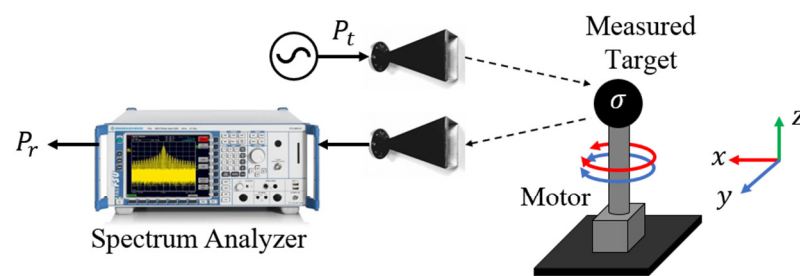


Figure 8. RCS Measurement System. This system comprises a transmitter with a specified transmission power P_t , a motor, and a spectrum analyzer. The motor is designed to rotate the target being measured along the x - and y -axes, facilitating comprehensive RCS analysis.

The RCSs of the objects depicted in Figure 9 were determined using the outlined steps. Calibration of the constant K was achieved with a metallic sphere (Figure 9b). The FS power measurement involved recording the returned power in the absence of both the target and the calibration object, a procedure vital for calibrating side effects.

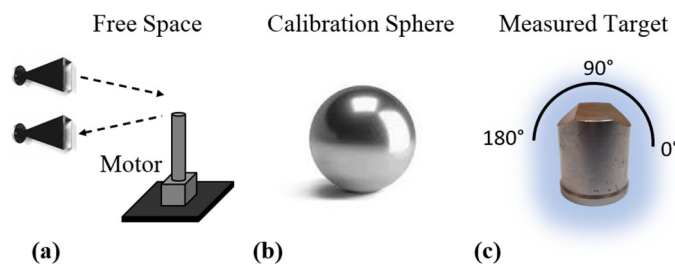


Figure 9. Objects for the RCS measurement procedure. The FS power in (a) is measured without any target or calibration object for side effect calibration. The calibration object in this study is a metal sphere (b). The measured target in this study was a metal object with a caliber of 20 mm, as presented in (c).

The motor depicted in Figure 9a features a one-degree resolution. Measurements were conducted on the front of a metal object, as shown in Figure 9c, across a range from 0° to 180° . Figure 10 displays the RCS results for the object, represented as a two-dimensional graph.

The measured object demonstrated five distinct wings with significant returns, mirroring the direction of transmission. These include one return at the front, two on each side, and two additional significant returns emanating from the object’s cylindrical portion. The RCS measurements distinctly captured these returns, providing clear evidence of their presence and characteristics.

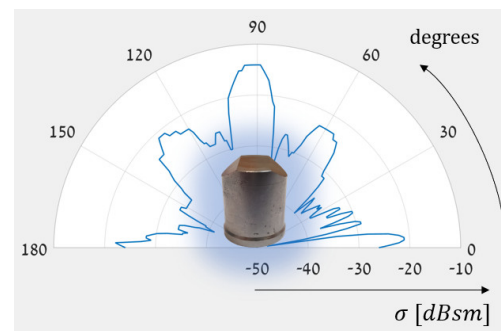


Figure 10. Measured RCS of a metal object. Measurements were taken from 0° to 180° and are presented in units of dBsm.

7. Summary and Conclusions

The results presented in the previous section demonstrate the effectiveness of our high-resolution millimeter-wave radar system in detecting and tracking high-speed objects with rapid acceleration capabilities. In this discussion, we explore the practical implications and potential real-world applications of our findings, situating our work within the broader context of radar technology and related fields. We also compare our results to those of previous studies, highlighting the novel contributions and advancements made by our research in the domain of civilian applications.

This research demonstrates the efficacy of high-resolution MMW radar for real-time detection and characterization of high-speed objects with rapid acceleration capabilities. Our experiments quantify the interplay between critical radar parameters and detection capabilities through live measurements of high-speed object launches. We confirm that high antenna directionality, as dictated by gain and beamwidth, is vital for maximizing detection range. Additionally, adopting an adequately high carrier frequency ensures short integration times for resolving the rapid velocity changes induced by the complex dynamics of these objects.

These empirical findings validate the uniqueness of MMW radar for extracting precise micro-Doppler signatures, even amidst substantial Doppler shifts beyond the scope of conventional microwave radar. By allowing accurate capture and analysis of complex target motions, MMW radar systems open new possibilities for various civilian applications requiring reliable tracking of maneuvering high-speed objects, such as in aerospace research, space exploration, meteorology, and safety systems. The ability to detect and track objects with rapid acceleration capabilities is crucial for developing advanced early warning systems, collision avoidance mechanisms, and space debris monitoring solutions.

Furthermore, the insights gained from this research contribute to the development of more sophisticated trajectory prediction models and algorithms that can be applied in air traffic management, weather forecasting, and scientific studies of high-speed phenomena. The detailed analysis of micro-Doppler signatures associated with rapidly accelerating objects provides valuable information for enhancing the accuracy and reliability of these models.

In comparison to previous studies that focused primarily on the detection of slower-moving targets or objects with constant velocities, our research pushes the boundaries of radar technology by successfully demonstrating the capability to detect and track objects with rapid acceleration and high velocities. This advancement opens up new avenues for scientific exploration and technological innovation in fields that require precise monitoring of fast-moving objects.

By presenting a comprehensive analysis of the performance of high-resolution MMW radar systems in detecting and tracking high-speed objects with rapid acceleration, our work lays the foundation for future research and development in this area. The findings of this study can be applied to optimize radar system design, improve signal processing

algorithms, and develop novel applications that leverage the unique capabilities of MMW radar technology in the civilian domain.

Author Contributions: Methodology, N.B.; Software, Y.R.; Validation, N.B.; Formal analysis, Y.R. and N.B.; Writing—original draft, Y.R. and N.B.; Writing—review & editing, N.B.; Supervision, N.B.; Project administration, N.B. All authors have read and agreed to the published version of the manuscript.

Funding: This research received no external funding.

Data Availability Statement: Data are contained within the article.

Conflicts of Interest: The authors declare no conflicts of interest.

References

1. Sutton, G.P.; Biblarz, O. *Rocket Propulsion Elements*; John Wiley & Sons: Hoboken, NJ, USA, 2016.
2. Balal, N.; Balal, Y.; Richter, Y.; Pinhasi, Y. Detection of Low RCS Supersonic Flying Targets with a High-Resolution MMW Radar. *Sensors* **2020**, *20*, 3284. [[CrossRef](#)] [[PubMed](#)]
3. Nenashev, V.A.; Shepeta, A.P.; Kryachko, A.F. Fusion Radar and Optical Information in MultiPosition On-Board Location Systems. In Proceedings of the 2020 Wave Electronics and its Application in Information and Telecommunication Systems (WECONF), St. Petersburg, Russia, 1–5 June 2020; pp. 1–5. [[CrossRef](#)]
4. Zhang, Q.; Luo, Y.; Chen, Y.-A. *Micro-Doppler Characteristics of Radar Targets*; Elsevier: Amsterdam, The Netherlands, 2016.
5. Rodrigues, D.V.Q.; Li, C. A review on low-cost microwave Doppler radar systems for structural health monitoring. *Sensors* **2021**, *21*, 2612. [[CrossRef](#)] [[PubMed](#)]
6. Abdu, F.J.; Zhang, Y.; Fu, M.; Li, Y.; Deng, Z. Application of deep learning on millimeter-wave radar signals: A review. *Sensors* **2021**, *21*, 1951. [[CrossRef](#)] [[PubMed](#)]
7. Kim, C.K.; Azim, M.T.; Singh, A.K.; Park, S.-O. Doppler shifting technique for generating multi-frames of video SAR via sub-aperture signal processing. *IEEE Trans. Signal Process.* **2020**, *68*, 3990–4001. [[CrossRef](#)]
8. Chen, V.C.; Li, F.; Ho, S.S.; Wechsler, H. Micro-Doppler effect in radar: Phenomenon, model, and simulation study. *IEEE Trans. Aerosp. Electron. Syst.* **2006**, *42*, 2–21. [[CrossRef](#)]
9. Rizvi, S.M.D.; Ahmad, S.; Khan, K.; Hasan, A.; Masood, A. Deep learning approach for fixed and rotary-wing target detection and classification in radars. *IEEE Aerosp. Electron. Syst. Mag.* **2022**, *37*, 32–42. [[CrossRef](#)]
10. Wang, J.; Jiang, C.; Zhang, H.; Ren, Y.; Chen, K.C.; Hanzo, L. Thirty years of machine learning: The road to Pare-to-optimal wireless networks. *IEEE Commun. Surv. Tutor.* **2020**, *22*, 1472–1514. [[CrossRef](#)]
11. Balal, Y.; Balal, N.; Richter, Y.; Pinhasi, Y. Time-frequency spectral signature of limb movements and height estimation using micro-doppler millimeter-wave radar. *Sensors* **2020**, *20*, 4660. [[CrossRef](#)] [[PubMed](#)]
12. Lei, P.; Liang, J.; Guan, Z.; Wang, J.; Zheng, T. Acceleration of FPGA based convolutional neural network for human activity classification using millimeter-wave radar. *IEEE Access* **2019**, *7*, 88917–88926. [[CrossRef](#)]
13. Buller, K. Identifying high velocity objects in complex natural environments using neural networks. *Procedia Comput. Sci.* **2016**, *95*, 185–192. [[CrossRef](#)]
14. Jha, U.S. The millimeter Wave (mmW) radar characterization, testing, verification challenges and opportunities. In Proceedings of the 2018 IEEE AUTOTESTCON, National Harbor, MD, USA, 17–20 September 2018; pp. 1–5.
15. Chen, V.C. *The Micro-Doppler Effect in Radar*; Artech House: New York, NY, USA, 2019.
16. Skolnik, M. An introduction and overview of radar. In *Radar Handbook*; McGraw Hill: New York, NY, USA, 2008.
17. Wan, M.; Sheng, J.; Ding, X.; Xing, M. Atmospheric Effects on Ultra-High-Resolution Millimeter-Wave ISAR Imagery for Space Targets. In Proceedings of the 2021 CIE International Conference on Radar (Radar), Haikou, China, 15–19 December 2021; pp. 142–145.
18. Wagner, T.; Feger, R.; Stelzer, A. Radar signal processing for jointly estimating tracks and micro-Doppler signatures. *IEEE Access* **2017**, *5*, 1220–1238. [[CrossRef](#)]
19. Ye, W.; Chen, H. Human activity classification based on micro-Doppler signatures by multiscale and multitask Fourier convolutional neural network. *IEEE Sensors J.* **2020**, *20*, 5473–5479. [[CrossRef](#)]
20. Ricci, R.; Balleri, A. Recognition of humans based on radar micro-Doppler shape spectrum features. *IET Radar Sonar Navig.* **2015**, *9*, 1216–1223. [[CrossRef](#)]
21. Bell, M.R. Information theory and radar waveform design. *IEEE Trans. Inf. Theory* **1993**, *39*, 1578–1597. [[CrossRef](#)]
22. Ritchie, M.; Fioranelli, F.; Borrión, H.; Griffiths, H. Multistatic micro-Doppler radar feature extraction for classification of unloaded/loaded micro-drones. *IET Radar, Sonar Navig.* **2017**, *11*, 116–124. [[CrossRef](#)]

23. Patel, J.S.; Fioranelli, F.; Anderson, D. Review of radar classification and RCS characterization techniques for small UAVs or drones. *IET Radar Sonar Navig.* **2018**, *12*, 911–919. [[CrossRef](#)]
24. Balal, Y.; Yarimi, A.; Balal, N. Non-Imaging Fall Detection Based on Spectral Signatures Obtained Using a Micro-Doppler Millimeter-Wave Radar. *Appl. Sci.* **2022**, *12*, 8178. [[CrossRef](#)]

Disclaimer/Publisher’s Note: The statements, opinions and data contained in all publications are solely those of the individual author(s) and contributor(s) and not of MDPI and/or the editor(s). MDPI and/or the editor(s) disclaim responsibility for any injury to people or property resulting from any ideas, methods, instructions or products referred to in the content.